Evolution and Complexity of Dental (Apatite-Based) Biominerals: Mimicking the Very Beginning in the Laboratory

Elena Rosseeva, Horst Borrmann, Raul Cardoso-Gil, Wilder Carrillo-Cabrera, Olga V. Frank-Kamenetskaya[1], Yigit Öztan, Yurii Prots, Ulrich Schwarz, Paul Simon, Andrey V. Zhuravlev[2], and Rüdiger Kniep

It is assumed that the major living organisms began to create mineralized hard tissues acting as functional materials around 525 Ma ago [1]. From this time up to now significant geological and biological changes have occurred, resulting in the development and evolution of different types of living organisms. Simultaneously, also the biological processes by which organisms create hard tissues in form of inorganic-organic nanocomposites have been optimized by natural selection through continuous evolution of animal phyla. As a result, mineralized hard tissues emerged which display fascinating hierarchical structures at different length scales and which are characterized by unique combinations of physical and mechanical properties. There are three basic inorganic components forming skeletal biomaterials: calcium carbonates, calcium phosphates (mainly in form of apatite) and silica. Besides this, in order to modify and develop biomaterials with specific properties, living organisms from different phyla developed the ability to involve other mineral types in biomineralization processes as well (already more than 64 different mineral phases have been reported) [1c]. In the present contribution, we focus on apatite-based biominerals which play a decisive role in the formation of endoskeletons (bone and teeth) of most vertebrates.

Paleobiologists suggest that phosphate biomineralization is quite unique in living systems. In contrast to calcium carbonate and silica biomineralization, which is widely spread in organisms from different phyla, calcium phosphate (apatite) skeletons are predominantly present only in vertebrates and some brachiopods [1]. Vertebrates, especially chordates, represent the most highly advanced and complex group of animals including fishes, amphibians, birds, mammals, etc. The development of hierarchical nanocomposite structures of hard tissues of bone and teeth is highly complex, involving processes of metabolism and cell activities. Bone hard tissue is a hybrid material composed of collagen and hydroxyapatite, where a close orientational relation between the triple-helical collagen macromolecules and the apatite nanoparticles is present. It is known that the *c* axis of apatite runs nearly parallel to the long axis of the protein macromolecules [2]. The mineralization of bone and dentine occurs under control of an organic matrix, which mostly contains collagenic proteins (about 90 wt.% of the complete organic part). In contrast, the main components of the enamel extracellular matrix are non-collagenic proteins (amelogenins and enamelins) [3]. In addition, besides the insoluble organic matrix which provides a scaffold for mineralization, the functional soluble organic molecules (such as amino acids, lipids, glycoproteins, etc.) also play an important role during the crystallization processes acting as crystal modifiers and controlling the shape and architecture of the growing composite materials.

The main inorganic component of the hard tissues (skeletons) of the most recent vertebrates (including humans) consists of carbonated hydroxyapatite, which contains only low concentrations of fluoride (less than 0.3 wt.%) [3a]. Fluorapatite, however, is present in dental enameloids of some fishes (e.g. shark) [4] and also in hard tissues of the feeding apparatus of conodonts – one of the earliest vertebrates [5]. The role of fluoride ions during biological mineralization of dental or dental-like hard tissues is not yet clearly understood. It is well known, however, that the presence of fluoride in the apatite component decreases its reactivity and its dissolution behavior (thus retarding the processes of demineralization) and at the same time increases the hardness of the materials [3a, 4b]. It is also assumed that the presence of fluoride "simplifies" the apatite crystal habit [6g]. On the other hand, it is not yet clear whether the decreasing fluoride content in the apatite component of dental hard tissues of higher vertebrates is due to evolutionary selection scenarios. In order to mimic apatite-based biomineralization processes we reduced the level of complexity by restricting the investigations on the formation of fluorapatite-gelatine nanocomposites grown by

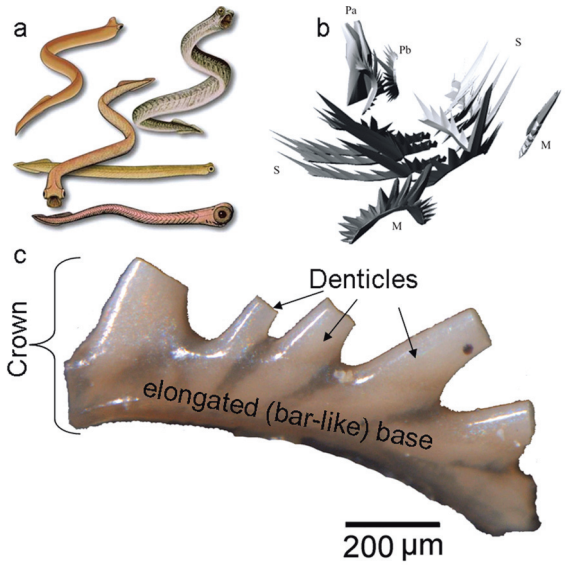

Fig. 1: (a) Reconstructions of conodont bodies (~ 4 cm in length), based on the imprint shapes of the soft-tissue conodont remains in limestone [5b]; (b) Reconstructed 3D model of the conodont feeding apparatus (genus *Youngquistognathus*) [5d, f]; (c) S-element of the feeding apparatus of *Polygnathus* conodonts (denticles are broken).

double diffusion in gelatine-gel matrices (excluding cell activities) [6]. By this, it was shown that the chemical composition of the as-grown materials is closely related to dental enameloid of sharks and even human enamel, although the latter contains hydroxyapatite instead of fluorapatite as inorganic component.

In the present contribution, we report on the results of our comparative investigations on the inner structure of conodont denticles and biomimetically grown fluorapatite-gelatine nanocomposite aggregates.

What are conodonts? Conodonts are small extinct marine animals (Fig. 1a) which inhabited a variety of environments in Paleozoic and Triassic seas [5]. Microscopic remains of conodonts can be found as so-called conodont elements representing fossilized tooth-like units of their feeding apparatus. The conodonts assignment has been the subject of various debates since their first discovery by C.H. Pander in 1859, because the hard tissues of their fossilized skeletal remains are very special and not typical for the known animal phyla [5c, e, i, k].

Most paleobiologists refer this group of animals to the chordates and even earliest vertebrates [5c, e–i]. Previous investigations demonstrated that the feeding apparatus of conodonts is composed of 15 to 19 discrete elements which are structurally divided into three parts, the so-called P-, S- and M-regions (Fig. 1b). The S-elements in the rear of the feeding apparatus are assumed to be least affected during conodonts life [5f]. The structure of conodont elements consists of two basic units: the crown and the underlying basal body. The crown typically comprises a combination of hyaline (or lamellar) tissue and albid (or white matter) tissue [5a, d, h] (Fig. 1c). Recent results also showed that the conodont hard tissues contain trace amounts of organic matter, and may represent remnant proteinaceous material [7c]. However, the exact architecture of conodont elements, their arrangement and function are still a matter of controversy.

Samples of S-elements of *Polygnathus* conodonts (used for our investigation) were obtained from Late Devonian deposits (Middle Frasnian ~ 380 millions years) at the south coast of the Ilmen Lake (Novgorod region, Russia). Specimens were extracted from limestone (bioclastic lenses) by use of the conventional buffered acetic acid technique. The Color Alteration Indexes (CAI) of the investigated conodont elements (Fig. 1c) ranged from 1 to 1.5 indicating mild fossilization conditions favoring the preservation of the organic components [7]. These findings are supported by the absence of specific bands in the Raman spectra [7b] corresponding to carbonized remains possibly produced by pyrolysis of the organic components.

Structural relations: paleobiogenic/biomimetic. As summarized in Figure 2 (left column) the whole denticle of a conodont S-element exhibits X-ray (electron) scattering properties representative for a single crystal, and even the crystal structure (fluorapatite) could be solved from the diffraction data. The lattice parameters of albid crown tissue apatite are close to that of stoichiometric synthetic fluorapatite [8]. The results of the structure refinements also demonstrate that there is no evidence for the presence of vacancies at the Ca-site. The observed splitting of the F-site can be caused by partial substitution of F^- by larger OH^- (or Cl^-) ions within the channels of the apatite crystal structure. Furthermore, by means of Raman spectroscopy it was shown that phosphate ions are only partially substituted by carbonate ions (B-type substitution, less than 2 wt.%). The same scattering properties have already been reported for the biomimetic

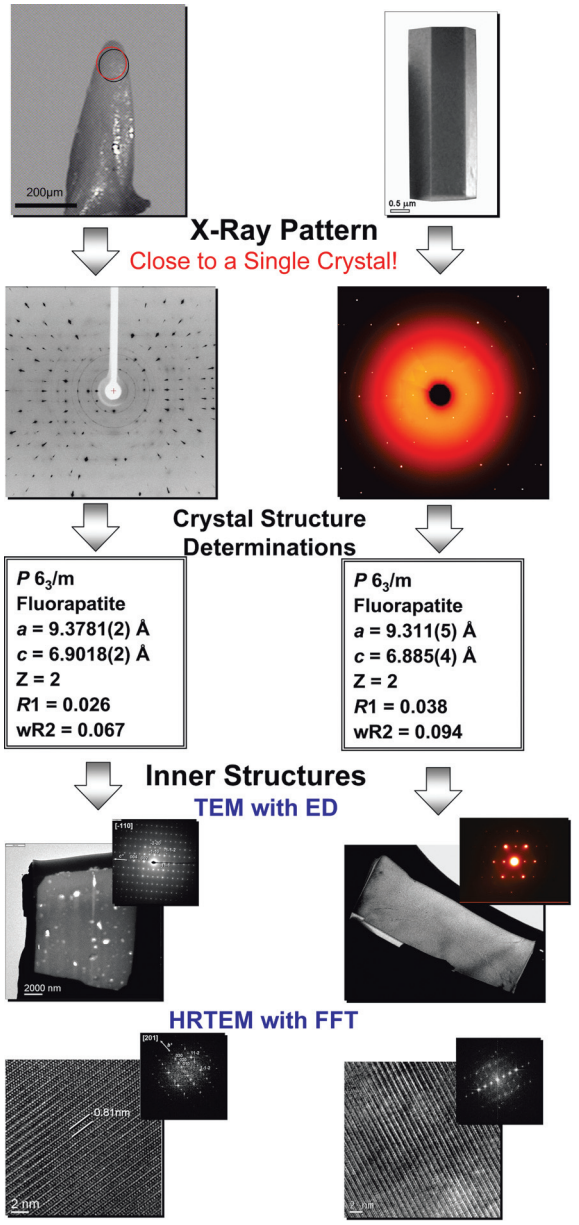

Fig. 2: Inner structure and scattering properties of a conodont S-element denticle (left column) and a hexagonal prismatic individual of biomimetic fluorapatite-gelatine nanocomposites (right column) [6g, i]. For further details see text.

hexagonal prismatic seeds of fluorapatite-gelatine nanocomposites (Fig. 2, right column). By means of SEM (Figs. 3a, b) and TEM (Fig. 2, left column, bottom) it was demonstrated that the denticle hard tissue is highly porous. The pores are varying in shape and size (from several nm to several µm). As can be seen from Figure 3 (c and d) a similar porous inner structure can also be obtained from the biomimetic fluorapatite-gelatine nanocomposites

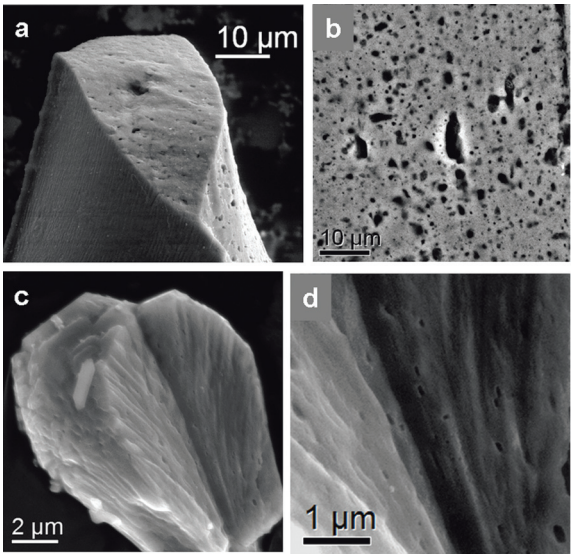

Fig. 3: (a,b) SEM images of the fracture area of a conodont S-element denticle, illustrating the porous inner structure of the albid crown tissue (white matter); (c) SEM image of a broken fluorapatite-gelatine composite aggregate after long-time heat treatment (800 °C, 24 h, Ar-atmosphere); (d) Zoomed image of (c) showing the presence of pores.

applying long-time heat treatment. In this case, the pores are formed at the former positions of integrated gelatine microfibrils, and/or are caused by recrystallization effects of the former nanocomposite building blocks (as a result of surface minimization [9b]).

The HRTEM images of FIB cuts of both the biomimetic and biogenic samples (Fig. 2, bottom) exhibit the crystal lattice of apatite as demonstrated by the FFT insets. By taking into account our experience with biomimetically grown fluorapatite-gelatine nanocomposites, we can conclude, that the materials under consideration represent highly mosaic-controlled nanocomposite superstructures [6]. This kind of materials is also classified as so-called “mesocrystals” [9]. For apatite-based biological hard tissues, the conodont denticle is the first remarkable example of such highly ordered mesocrystalline material. In addition, earlier TEM investigations of *J. A. Trotter et al.* [5h] demonstrated that in case of *Plectodina* conodonts, the tissue within the boundary area between the basal body and the hyaline crown consists of elongated nanocrystalline carbonated fluorapatite building blocks in more or less parallel alignment with respect to each other (Fig. 4a). Biomimetically grown carbonated fluorapatite-gelatine composite

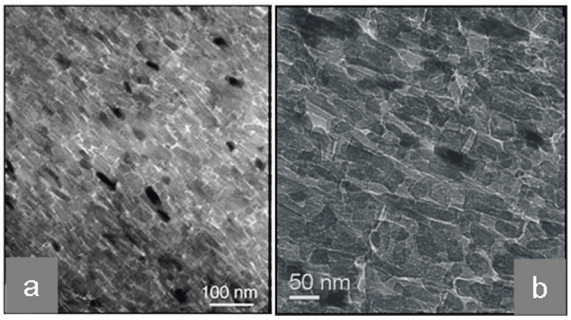

Fig. 4: (a) TEM image of an argon ion-milled thin section of the boundary area between the basal body and the hyaline crown tissue of *Plectodina* conodont [5h], showing nearly parallel alignment of elongated nano-sized building blocks; (b) TEM image of an ultra thin slice of a biomimetic carbonated fluorapatite-gelatine composite (carbonate content: ~ 4 wt.%) [6h] indicating the close structural relationship to (a).

aggregates are characterized by a similar inner structure [6h] shown in the TEM image (Fig. 4b) of an ultra thin slice (carbonate content: ~ 4 wt.%), indicating the presence of small elongated subunits with preferred orientation along crystallographic [001] direction. The length of the subunits is in the range between 60 nm and 100 nm.

As shown in Figure 5 (left column, a, b) the conodont elements can be decalcified by treatment with HCl (0.1 M). The gelatineous residue keeps the shape of the former individual, an observation which was also made for decalcified fluorapatite-gelatine nanocomposite individuals (Fig. 5, right column, a, b) [6a, g, h]. In analogy to the biomimetic nanocomposite aggregates (Fig. 5 right column, c, d) [6e–i], the existence of mineralized organic fibrils within a conodont denticle (FIB cut) can be shown by TEM (regions of lower density with varying diameters between 1.5 nm and 7 nm in Figure 5, left column, c). Furthermore, bundling of organic fibrils is visible in TEM images of partly decalcified conodont elements (Fig. 5, left column, d).

Preliminary investigations were already focused on the characterization of the organic component of conodont elements by means of gel electrophoresis (SDS PAGE). As a first result, it can be assumed, that the organic component is closely related to collagen-like proteins. Collagen is the main organic component of bone, dentine and enameloid of most recent vertebrates [1–3, 7c]. Further investigations are needed in order to prove these findings and to get more detailed information on the nature of the organic component within the conodont elements.

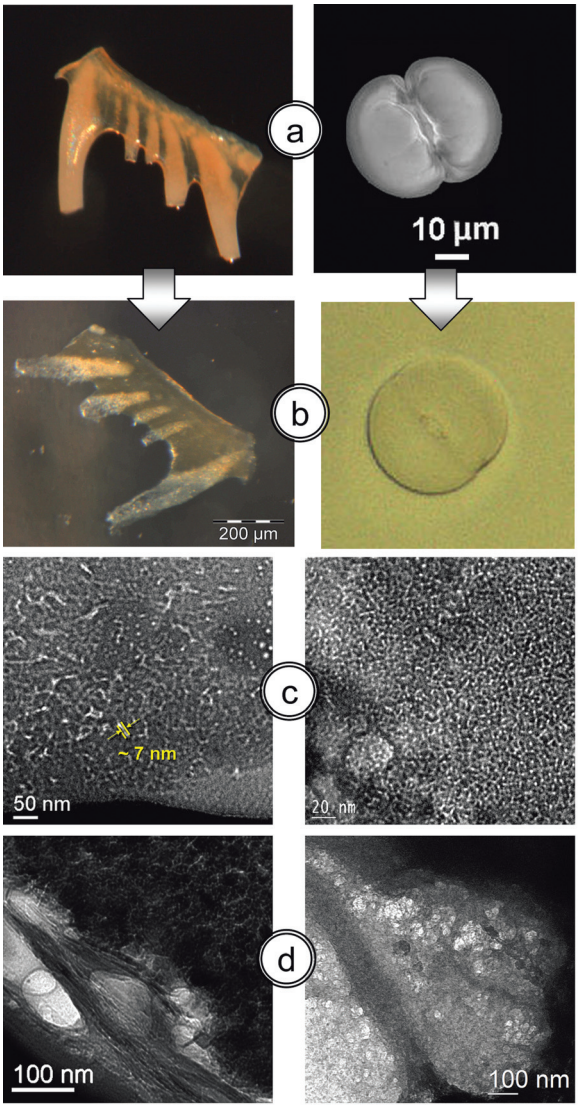

Fig. 5: Overview of the distribution of organic components within conodont elements and biomimetic fluorapatite-gelatine nanocomposite aggregates. (a) (left) S-element of a *Polygnathus* conodont feeding apparatus; (right) SEM image of a typical fluorapatite-gelatine nanocomposite sphere aggregate; (b) Completely decalcified gelatineous residue of a conodont element (HCl, 0.1 M) (left) and a biomimetic spherical aggregate (EDTA, 0.25M) (right); (c) TEM image of the FIB cut of a conodont denticle (left) and of a biomimetic aggregate (right) illustrating the presence of mineralized organic fibrils; (d) TEM images of the partly decalcified surface area of a conodont denticle (left) and decalcified gelatine residue of biomimetic aggregate (right) showing bundles of organic fibrils.

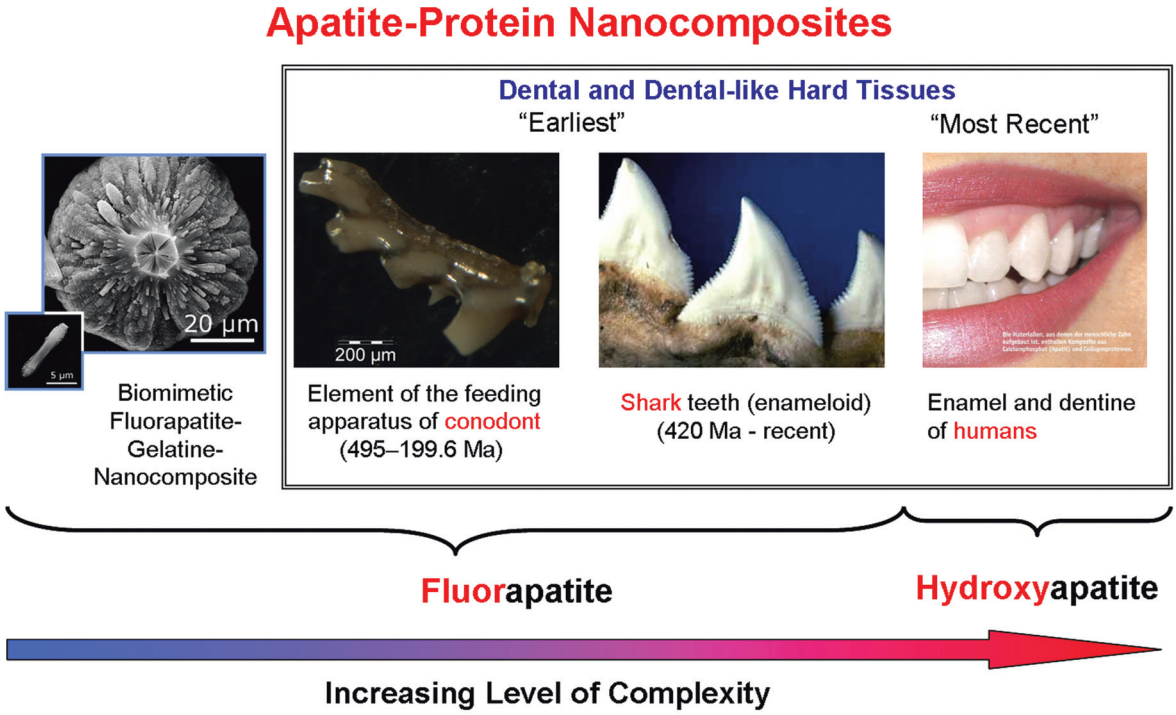

Fig. 6: Schematic illustration of evolutionary dentition developments. From fluorapatite- to hydroxyapatite- nanocomposites. Here, conodont elements and biomimetic fluorapatite-gelatine composites represent the lowest level of complexity. For further details see text.

Summary

During evolution of vertebrate dentition, natural selection processes probably started from the development of denticles (lower vertebrates) composed of fluorapatite-organic composites closely related to single crystals (highly oriented nanocomposite building blocks). This situation was followed by formation of enameloid hard tissues with less ordered and smaller fluorapatite-organic composite nanoblocks (teeth of some fishes, e.g. sharks [4]) and finally led to development of dental enamel (higher vertebrates) composed of even less ordered hydroxyapatite-organic nanocomposite building blocks [3]. This evolutionary process caused the formation of dental hard tissues (e.g. enamel) which are characterized by lower hardness, but by a significantly increased elasticity and toughness (recently also proven by atomistic simulations of pseudo-elastic deformation and self-healing processes of apatite-collagen composites [10,11]).

Figure 6 shows a schematic illustration of evolutionary dentition developments. Conodont elements belong to the fluorapatite group and take the position of the lowest level of complexity in this representation. The most interesting result of our investigations on conodont elements and biomimetic fluorapatite-gelatine nanocomposites refers to the close relationships between the biogenic and biomimetic composite structures on various length-scales (from nm up to µm), and to the fact that the biomimetic nanocomposite is grown without cell activities, just by interaction and self-organization of the basic chemical components. This observation builds the bridge between paleobiology (early development of vertebrates) and today's experiments in the laboratory, and holds the chance to get deeper insight into general principles of very early scenarios in biomineralization.

References

[1] (a) *H. Knoll,* Rev. in Miner. and Geochem. **54** (2003) 329; (b) *A. L. Boskey* , Elements. **3** (2007) 385; (c) *P. M. Dove* , Elements. **6**(1) (2010) 37.

[2] *M. J. Glimcher,* Rev. in Miner. and Geochem. **64** (2006) 223.

[3] (a) *J. C. Elliott*, Rev. in Miner. and Geochem. **48** (2002) 427; (b) *M. Golberg, D. Septier, S. Lecolle, H. Chardin, M. A. Quintana, A. C. Acevedo, G. Gafni, D. Dillouya, L. Vermelin, B. Thonemann, G. Schmalz, P. Bissilamapahou, and J. P. Carreau*, Int. J. Dev. Biol. **39** (1995) 93.

[4] (a) *R. Z. LeGeros, P. Go, and S. Suga,* J. Dent. Res. **57 (**1978) 280; (b) *R. Z. LeGeros, L. M. Silverstone, G. Daculsi, and L. M. Kerebel,* J. Dent. Res. **62(2)** (1983) 138; (c) *Y. Miake, T. Aoba, E. C. Moreno, S. Shimoda, K. Prostak, and S. Suga.* Calcif. Tissue Int. **48** (1991) 204.

[5] (a) *P. C. J. Donoghue* Philos. Trans. Royal Soc. London, **B 353** (1998) 633; (b) *M. A. Purnell*, Univ. of Leicester, 1999, http://www.le.ac.uk/geology/map2 /abstractsetc/cavhet.html; (c) *W. C. Sweet, P. C. J. Donoghue*, J. Paleont. **75(6)** (2001) 1174; (d) *A.V. Zhuravlev,* Late Palaeozoic conodont element histology and micro-ornamentation. St. Petersburg, 2002, 94 (in Russian); (e) *P. C. Donoghue, I. J. Sansom, and J. P. Downs*, J. Exp. Zoolog. B Mol. Dev. Evol. **306** (2006) 278; (f) *A.V. Zhuravlev,* Paleo. J. **5** (2007) 75; (g) *J. A. Trotter, and S. M. Eggins,* Chemical Geology. **233** (2006) 196; (h) *J. A. Trotter, J. D. Fitz, H. Kokkonen, and C. R. Barnes,* Lethaia **40** (2007) 97; (i) *K. Kawasaki, A. V. Buchanan, and K. M. Weiss,* Annu. Rev. Genet. **43** (2009) 119; (k) *S. Turner, C. J. Burrow, H. -P. Schultze, A. Blieck, W.-E. Reif, C. B. Rexroad, P. Bultynck, and G. S. Nowlan*, Geodiversitas. **32(4)** (2010) 545.

[6] (a) *R. Kniep, and S. Busch,* Angew. Chem. **108** (1996) 2787; Angew. Chem. Int. Ed. **35** (1996) 2624; (b) *S. Busch, H. Dolhaine, A. DuChesne, S. Heinz, O. Hochrein, F. Laeri, O. Podebrand, U. Vietze, T. Weiland, and R. Kniep,* Europ. J. Inorg. Chem. **10** (1999) 1643. (c) *S. Busch, U. Schwarz, and R. Kniep*, Chem. Mater. **13** (2001) 3260; (d) *S. Busch, U. Schwarz, and R. Kniep,* Adv. Funct. Mater. **13** (2003) 189; (e) *P. Simon, W. Carrillo-Cabrera, P. Formanek, C. Göbel, D. Geiger, R. Ramlau, H. Tlatlik, J. Buder, and R. Kniep*, J. Mater. Chem. **14** (2004) 2218; (f) *P. Simon, U. Schwarz, and R. Kniep,* J. Mater. Chem. **15** (2005) 4992; (g) *R. Kniep, and P. Simon*, Top. Curr. Chem. Springer. **270** (2007) 73; (h) *E. V. Rosseeva, J. Buder, P. Simon, U. Schwarz, O. V. Frank-Kamenetskaya, and R. Kniep,* Chem. Mat. **19** (2008) 6003; (i) R. *Kniep, and P. Simon*, Angew. Chem. **120** (2008) 1427; Angew. Chem. Int. Ed. **47** (2008) 1405; (f) *E. V. Rosseeva*, St. Petersburg, State Univ., Diss. 2010, 209.

[7] (a) *C. P. Marshall, H. R. Rose, G. S. H. Lee, G. L. Mar, and M. A. Willson,* Organ.Geochem. **30** (1999) 1339; (b) *C. P. Marshall, G. L. Mar, R. S. Nicoll, and M. A. Wilson* Organ. Geochem. **32** (2001) 1055; (c) *A. Kemp,* J. Paleont., **76(3)** (2002) 518.

[8] *K. Sudarsan, R. A. Young, P. E. Mackie,* Mat. Res. Bull. **7(11)** (1972) 1331.

[9] (a) *H. Cölfen, and M. Antonietti,* Angew. Chem. **117** (2005) 5714; Angew. Chem. Int. Ed. **44** (2005) 5576; (b) *H. Cölfen, and M. Antonietti,* Mesocrystals and Nonclassical Crystallization, Wiley, 2008.

[10] (a) *D. Zahn*, Comput. Mater. Sci. **45** (2009) 845; (b) *D. Zahn*, J. Chem. Phys. **128** (2008) 184707; (c) *D. Zahn*, Angew. Chem. Int. Ed. **49** (2010) 9405; Nature Materials, **9** (2010) 958.

[11] *D. Zahn et al.,* in Scientific Report 2009–2010, p.177 (Max Planck Institute for Chemical Physics of Solids, Dresden, Germany, 2011)

---

[1] Saint Petersburg State University, Saint Petersburg, Russia

[2] All-Russian Research Petroleum Exploration Institute of the Ministry of Natural Resources of the Russian Federation (VNIGRI), Saint Petersburg, Russia